Modelling the high-resolution dynamic exposure to flood in city-region

Xuehong Zhu[1], Qiang Dai[1, 2, *], Dawei Han[2], Lu Zhuo[2], Shaonan Zhu[3], Shuliang Zhang[1, *]

[1]Key Laboratory of VGE of Ministry of Education, Nanjing Normal University, Nanjing, China

[2]WEMRC, Department of Civil Engineering, University of Bristol, Bristol, UK

[3]College of Geographical and Biological Information, Nanjing University of Posts and Telecommunications, Nanjing, China

*Correspondence: q.dai@bristol.ac.uk

Abstract:

Urban flooding exposure is generally investigated with the assumption of stationary disasters and disaster-hit bodies during an event, and thus cannot satisfy the increasingly elaborate modelling and management of urban floods. In this study, a comprehensive method was proposed to simulate dynamic exposure to urban flooding considering residents' travel behavior. First, a flood simulation was conducted using the LISFLOOD-FP model to predict the spatio-temporal distribution of flooding. Second, an agent-based model was used to simulate residents' movements during the urban flooding period. Finally, to study the evolution and patterns of urban flooding exposure, the exposure of population, roads, and buildings to urban flooding was simulated using Lishui, China as a case study. The results showed that urban flooding and population distribution had evident spatio-temporal variations. Additionally, the exposure increased with increasing rainfall intensity and flooding extent. The urban area near the Oujiang River was the most severely flooded, resulting in the highest exposure of population, roads, and buildings. Furthermore, the impacts of flooding on roads were greater than those on the population and on buildings. This study presents the first fully formulated method for dynamic urban flood exposure simulation at a high spatio-temporal resolution. The quantitative results of this study can provide fundamental information for urban flood disaster vulnerability assessment, socioeconomic loss assessment, urban disaster risk management, and emergency response plan establishment.

26 **Keywords:** urban flooding; resident travel behavior; agent-based model; dynamic exposure

1. Introduction

28 Storm flooding has become increasingly frequent and severe with the intensification of global

29 warming and the rising frequency of extreme weather events (*Dankers and Feyen, 2008*;

30 *Hammond et al., 2015*). Urban floods have become major natural disasters in many cities around

31 the world and have created serious threats to human life and social and economic activities (*Gain*

32 *et al., 2015*). Effectively coping with floods and their adverse effects is an important part of disaster

33 prevention and mitigation as well as disaster risk management (*Atta-Ur-Rahman, 2014*). Non-

34 engineering measures such as exposure assessment are currently the main way of managing urban

35 flooding risk (*Chen et al., 2015*). Exposure refers to the presence of people, livelihoods,

36 environmental services and resources, infrastructure, or economic, social, or cultural assets in

37 places that could be adversely affected by natural disasters (*IPCC, 2012*). Urban flood disasters

38 are caused by the adverse effects of heavy rain and other factors on the city system in certain

39 disaster-prone environments. These events consist of three parts: disaster-causing factors, disaster-

40 prone environments, and disaster-hit bodies (*Shi, 1996*).

41 The characteristics of flood disasters and building environments and the distribution of population

42 and socio-economic resources are the key factors for evaluating urban flood exposure due to the

43 dynamic evolution of urban floods and disaster-hit bodies. The methods used for evaluating

44 exposure to urban flooding at a certain time or period vary due to changes in the disaster-hit bodies,

45 study areas, and data acquisition methods (*Röthlisberger et al., 2017*). Index-based methods are

46 commonly used for comprehensive exposure evaluation (*Mahe et al., 2005*; *Mansur et al., 2016*;

47   *Guo et al., 2014*). Statistical methods based on historical disaster data are also utilized (*Moel et al.,*

48   *2011*).

49   With respect to spatial considerations, the currently implemented method for estimation of disaster

50   exposure adopts the administrative boundaries of socioeconomic data, which are organized as

51   research units (*Yin, 2009*). Consequently, natural elements that have higher spatial resolutions must

52   be compromised due to the lower spatial resolution of human elements like population (*Yang et*

53   *al., 2013*). Therefore, a comprehensive and sophisticated geographic research unit has not been

54   established, thus resulting in simulation results applicable only to macro-scale planning and

55   decision making. Hence, the estimation of disaster exposure needs to incorporate greater spatial

56   heterogeneity and resolution.

57   Besides enhancement of the spatial scale, dynamic temporal simulation of disaster exposure has

58   gained increasing attention. Specifically, the dynamic evolution of disaster exposure at the macro

59   time scale considers exposure distribution as well as its variation during different development

60   periods (*Weis et al., 2016*). Therefore, this method is relatively mature and has led to abundant

61   research results. At the micro time scale, disaster-causing factors and disaster-hit bodies

62   represented by populations are constantly varying. On one hand, spatio-temporal changes in

63   disaster-causing factors (rainfall) result in corresponding dynamic changes in the characteristics

64   (water depth and velocity) of urban flood disasters. On the other hand, daily travel activities of

65   urban residents, such as commuting between residential and work or study areas, cause a dynamic

66   spatio-temporal distribution of the population. At the same time, the exposure to urban flooding

67   changes dramatically over a short period of time. To avoid or reduce disaster risks, casualties, and

68   property losses, different individuals are likely to adopt different adaptive behaviors, such as

69   delaying or cancelling travel plans, while the government is likely to adopt organizational actions

70   such as issuing warnings and evacuating residents (*Wan and Wang, 2017*; *Parker et al., 1995*).

71   Thus, the dynamic simulation of exposure requires the dynamic space-time simulation of

72   variations in the disaster, and disaster-hit bodies, as well as interactions between them.

73   Modelling of the spatio-temporal changes in natural disasters mainly uses the disaster system

74   simulation method, such as the hydrological or hydrodynamic models used to simulate flood

75   disasters (*Werren et al., 2016*). The change simulation of the disaster-hit body (population) can

76   use methods based on individual space-time data (*Liang et al., 2015*) and the agent-based method

77   (*Kang et al., 2012*). Although the former can acquire human positions and movement tracks, it is

78   difficult to identify the purpose of human activities, and human disaster response behavior cannot

79   be simulated. The agent-based model (ABM) can not only simulate the population distribution but

80   can also simulate the interaction among the population (as the disaster victim), the hazard factors,

81   and the disaster-prone environment (*Yin, et al., 2016b*). Current research has used the ABM to

82   simulate human responses to disasters, which, in turn, have been used in natural disaster risk

83   research (*Johnstone, 2012*; *Huang et al., 2015*). Nevertheless, the simulation results do not reflect

84   the exposure characteristics of the disaster-hit bodies and their dynamic changes (*Dawson et al.,*

85   *2011*).

86   Therefore, the objectives of this study were to develop a novel method using the LISFLOOD-FP

87   model (Sect. 3.1) and an ABM (Sect. 3.2) to simulate the exposure of urban populations, roads,

88   and buildings to flooding under varying conditions and subsequently implement the method as a

89   pilot in a real city. Several scenarios, including diverse flooding types and various responses of

90   residents to flooding, were considered in this regard. Additionally, dynamic features of the real

91   world were incorporated to improve the micro exposure analysis. This method was subsequently

92   applied to an urban area as a case study. Exposure simulation is a useful tool for estimating disaster

93   vulnerability and assessing losses, and the quantitative results under different scenarios of this

94   study are likely to benefit relevant government agencies in assessing risk, issuing warnings, and

95   planning emergency responses to urban natural disasters. In particular, considering the dynamic

96   distribution of the population under flooding, a more reasonable mitigation measure can be taken

97   to minimize casualties.

98   **2.   Study area and data source**

99   In this study, Lishui City in Zhejiang Province, China, was considered as the study region because

100   of the availability of the required data and flooding history. The urban district of Lishui is a largely

101   hilly and mountainous area, and the Oujiang River traverses its southern and eastern parts. The

102   study area is located in the central district of Lishui, covers an area of 43.4 km^2, and has a large

103   population of about 71673 (Fig. 1). The frequencies of heavy rainstorms and persistent

104   concentrated rainfall events rise sharply in May and June during the Meiyu flood period, which

105   often results in flood disasters. On August 20, 2014, a heavy rainfall event lasting a few days

106   produced a 50-year flood in Lishui and caused considerable loss of property.

107   The datasets used in this study included a digital elevation model, rivers, roads, buildings,

108   population, and observation data consisting of river discharge and water level. Travel survey data

109   were used to generate daily routines. Additionally, traffic flow and water accumulation data were

110   used for validation. Table 1 describes the sources and uses of the datasets.

111   The travel survey data used in this study were taken from a face-to-face questionnaire survey

112   conducted from July 8, 2018 to July 14, 2018. A total of 25 subdistricts were selected based on

113   sample selection. According to the distribution of the subdistricts, the investigators were divided

114   into five groups of at least four investigators per group. In each group, a senior researcher

115   monitored the survey process, coordinated questionnaire collection and checked the completeness

116   and validity of the questionnaires collected. Before each interview, the investigators explained the

117   purpose of the investigation and confidentiality principles. The respondents in the study

118   participated voluntarily, and were allotted enough time to answer the questionnaire. In total, 623

119   questionnaires were distributed, 589 were collected, and 500 valid responses were selected after

120   excluding incomplete questionnaires (the response rate was 80.3%). The distribution of the social

121   characteristics of the respondents coincided with the actual population distribution in the study

122   area.

123   **3. Methodology**

124   This study comprised three aspects: disaster simulation, human activity simulation, and dynamic

125   exposure assessment (Fig. 2). The first step included fluvial and pluvial flooding simulation based

126   on the LISFLOOD-FP model. The simulation of human activity utilized ABM to obtain the spatio-

127   temporal distribution of the population under different scenarios. Finally, the developed model

128   was combined with the results of the previous two steps to assess the dynamic exposure of the

129   population, roads, and buildings to urban flooding.

130   **3.1 Flood models**

131   A wide variety of existing hydrological or hydrodynamic models capable of simulating fluvial or

132   pluvial flooding are available; these include the Storm Water Management Model (SWMM)

133   (*Rossman, 2015*), LISFLOOD (*Bates and De Roo, 2000*), MIKE-SHE (*DHI, 2000*), MIKE-11

134   (*Havnø et al., 1995*), MOUSE (*Lindberg et al., 1989*), HEC-RAS (*Brunner, 2008*), and HEC-HMS

135   (*Charley et al., 1995*). LISFLOOD-FP (*Bates et al., 2013*) is a coupled 1D/2D hydraulic model

136   based on a raster grid and was designed for research purposes at the University of Bristol.

137   LISFLOOD-FP uses a square grid as the computational grid to simulate one-dimensional river

138   hydraulic changes and two-dimensional floodplain hydraulic changes. The applicability of the

139   model has been verified by several studies (*Horritt and Bates, 2002*; *Bates and De Roo, 2000*).

140   Therefore, the LISFLOOD-FP model was chosen for the simulation of fluvial and pluvial flooding.

141   Floodplain flows were described in terms of the continuity and momentum equations discretized

142   over a grid of square cells, which allowed the model to represent 2D dynamic flow fields for the

143   floodplain. It assumed that the flow between two cells was simply a function of the free surface

144   height difference between those cells:

145     $\dfrac{dh^{i,j}}{dt} = \dfrac{Q_x^{i-1,j} - Q_x^{i,j} + Q_y^{i,j-1} - Q_y^{i,j}}{\Delta x \Delta y}$,   (1)

146     $Q_x^{i,j} = \dfrac{h_{flow}^{5/3}}{n} \left(\dfrac{h^{i-1,j} - h^{i,j}}{\Delta x} \right)^{1/2} \Delta y$,   (2)

147   where $h^{i,j}$ is the free surface height of water at node (*i,j*), Δx and Δy are the cell dimensions, n is

148   the effective grid scale Manning's friction coefficient for the floodplain, and Q_x and Q_y describe

149   the volumetric flow rates between the floodplain cells in the x and y directions, respectively. The

150   flow depth, h_{flow}, represents the depth through which water can flow between two cells, and d is

151   defined as the difference between the highest free surface height of water in the two cells and the

152   highest bed elevation.

153   The types of flooding simulated in this study included pluvial and fluvial floods. The input of the

154   model included DEM, rainfall, channel, and floodplain friction data. When it comes to fluvial

155   flooding simulations, boundary conditions, including river, water level, and river discharge were

156   also needed. The output data were water depth and water velocity in the x and y directions,

157   respectively. Due to the lack of hourly rainfall observation data, we used designed rainfall data for

158   pluvial flood simulation. Synthetic rainfall data for a return period of 50 years were simulated

159   using the Chicago hyetograph method (CHM) (*Cen et al., 1998*). The rainfall data were determined

160   using the rainstorm intensity formula (Eq. (3)), rainfall duration time (T), and peak position (r).

161    $i = \frac{A(1+c\log P)}{167(t+b)^n},$ (3)

162   where i is the rainfall intensity (mm/min), P is the return period, and t is the time. A, b, c and n

163   are parameters related to the characteristics of the local rainstorm and need solutions. A is the

164   rainfall parameter, i.e. the design rainfall (mm) for 1 min at a 10 year return period, c is the rainfall

165   variation parameter (dimensionless), and b is the rainfall duration correction parameter, i.e. the

166   time constant (min) that can be added to convert the curve into a straight line after logarithmic

167   calculation of the two sides of the rainstorm intensity formula. n is the rainstorm attenuation index,

168   which is related to the return period. The "r" refers to the relative rainfall peak time, i.e., the value

169   from zero to one. Zero means the maximum rainfall at the beginning of rainfall and one means the

170   maximum rainfall at the end of rainfall. To simulate the flood in 2014, we fixed r at 0.2 based on

171   the assumption that the peak is located at the one fifth point of the design hyetograph. Additionally,

172   the rainfall duration was 6 hours (6 am to 12 pm), and the accumulated rainfall was 148.59 mm.

173   The parameters A, b, c and n were estimated from the rainstorm intensity formula for Lishui City

174   obtained from the "Zhejiang City Rainstorm Intensity Formula Table" published by the Hangzhou

175   Municipal Planning Bureau (Table 2). The rainfall simulation results are shown in Fig. 3(a). The

176   river discharge and water level input data for fluvial flood simulation utilized observational data

177   from Lishui's 50-year flood in 2014, provided by the Liandu Hydrological Station (Fig. 3(b)). The

178   flow data for the Daxi and Haoxi on August 20, 2014 were obtained from the Xiaobaiyan and

179   Huangdu stations, respectively, and the observational data for water levels at the outlets were those

180   for the Kaitan Dam.

181   **3.2 ABM**

182   Several modelling techniques, often collectively referred to as social simulation, have been

183   successfully used to represent the behaviors of humans and organizations. These include event and

184   fault trees, Bayesian networks, microsimulation, cellular automata, system dynamics, and ABMs.

185   Research methods based on ABMs have been gradually introduced to the field of natural disaster

186   risk assessment. ABM is considered most suitable to address challenges associated with simulating

187   the complexity and dynamic variability of population exposure to flooding due to its capacity to

188   capture interactions and dynamic responses in a spatial environment (*Dawson et al., 2011*).

189   An ABM is a computational method for simulating the actions and interactions of autonomous

190   decision-making entities in a network or system to subsequently assess their effects on the system

191   as a whole. Individuals and organizations represent agents. Each agent individually assesses its

192   situation and makes decisions based on a set of rules. Agents may execute various behaviors

193   appropriate for the system component they represent—for example, producing or consuming.

194   Therefore, an ABM consists of a system of agents and the relationships between them. Even a

195   simple ABM can exhibit complex behavior patterns because a series of simple interactions

196   between individuals may result in more complex system-scale outcomes that could not have been

197   predicted just by aggregating individual agent behaviors.

198   The ABM was developed as a concept in the late 1940s, and substantial applications were realized

199   with the emergence of high-powered computing. Such applications include those in the political

200   sciences (*Axelrod, 1997*), management and organizational effectiveness, and the behavior of social

201 networks (*Sallach and Macal, 2001*; *Gilbert and Troitzsch, 2005*). In recent years, it has been

202 introduced to the geosciences and other fields to provide novel ideas for the study of modern

203 geography, including land use simulation and planning as well as residential choice and residential

204 space differentiation (*Benenson et al., 2002*). The urban flood disaster system is a typical complex

205 "natural and social" system. The introduction of ABM to simulate space-time distributions of

206 populations is expected to quantify the dynamic exposure of populations to urban flood disasters.

207 For example, *Dawson et al. (2011)* proposed a dynamic ABM for flood event management to

208 evaluate population vulnerability under different storm surge conditions, dam break scenarios,

209 flood warning times, and evacuation strategies.

210 **3.3 Spatio-temporal simulation of population distribution**

211 The ABM of residents' travels established in this study included two core elements (agents and

212 activities) and two basic elements (blocks and networks). Individual movements were simulated

213 by defining the activity patterns of different types of residents, allowing us to obtain the

214 distribution of the population at each moment.

215 Residents were independent individuals with subjectivity, abstracted as agents in this study. Only

216 a limited number of agent classifications were used to reduce the number of agent types. The types

217 of agents were classified according to the social characteristics of the residents. Age and gender

218 characteristics mainly affect the ability of people to respond to disasters. The self-help abilities of

219 minors under 18 years of age and residents older than 60 years are generally poor. In the event of

220 natural disasters, they are generally categorized as the objects of help. The middle-aged group (18–

221 60 years old) generally has greater physical strength with a better ability to cope with disasters.

222 Unemployed people are more vulnerable to natural disasters. On one hand, their living

223   environments and resistance to disasters are poor; on the other hand, their economic conditions are

224   limited, which impedes recovery after the disaster and seriously affects their daily life in the short

225   term. Education level is related to the possibility of receiving early warning information by the

226   individual. Individuals with higher education levels are more likely to respond to early warning

227   information and are more aware of disasters than others (*Terti et al., 2015; Shabou et al., 2017*).

228   Additionally, different travel modes have different effects on the activity patterns of people as well

229   as on exposure levels when disasters occur. Therefore, the agent types were divided according to

230   age, gender, employment status, education level, and travel mode.

231   Activities were classified as work, study, recreation, shopping, at-home, and travel. An activity

232   pattern consisted of a series of activities to describe the spatio-temporal distribution of the agent.

233   The location and scope of an agent were restricted to blocks and networks. Different types of

234   agents indicated different activity patterns, and the same agent type could also indicate different

235   activity patterns in different scenarios. The travel survey data were used according to the

236   demographic properties of the agent to generate synthetic daily routines. To capture the variability

237   in the travel survey and the uncertainties in behavior, synthetic daily routines were described in

238   probabilistic terms. Figure 4 presents an example of the synthetic daily routine of an agent with

239   the following demographic characteristics: male agent, aged 18–60 years, and employed. In this

240   example, the agent started the day at 8 am on a weekday. The agent then had a 0.8 probability of

241   going straight to work, subsequently went home, and so on.

242   The study area was discretized into many blocks to improve the spatial resolution of the exposure

243   results. The major factors that affect the flood exposure are considered, including rivers, roads,

244   land use, and buildings. The discretization procedure was conducted with geographic information

245   system (GIS) tools (intersection and editing tools of the ArcGIS software) (*Lü et al., 2018*). Blocks

246   were activity places for agents and represented the smallest unit of exposure. This study divided

247   the block into five categories: residential area, school, company, recreational area and river.

248   Additionally, the residential areas were subdivided into I, II, III, and IV classes according to the

249   type of building.

250   In this study, the network referred to roads and restricted the spatial travel scope of an intelligent

251   agent. Rural roads, highways, and urban roads (including main roads, sub trunk roads, and its

252   branches) were included in the network. The route selection criteria were defined once the different

253   activities from each individual's schedule were located, and road section attributes were specified.

254   Although various factors are involved in the route choice process, several studies have indicated

255   that minimizing travel time is the principal criterion for selecting routes (*Papinski et al., 2009*;

256   *Ramming, 2001*; *Bekhor et al., 2006*). Here, a simple but effective shortest path method was used.

257   The classical Dijkstra algorithm is a single-source shortest path algorithm that provides trees of

258   minimal total length and time in a connected set of nodes (*Dijkstra, 1959*). The activity pattern

259   attributions concerned only the starting times and durations of the activity sequences, thus

260   indicating that the travel duration for each individual was computed based on the distance between

261   the different activity locations. Therefore, the implemented schedules may be distorted compared

262   to the assigned schedules in terms of travel durations (*Terti et al., 2015*). We can get the departure

263   and destination block of each stage according to the activity patterns, and then calculate the shortest

264   path consisting of a series of road sections. At each moment, the block in which the agent is located

265   is calculated. If on the road, according to differences in the speed of walking, riding a bus, or

266   driving a car, the road section location is calculated. During flooding, this is similar in every aspect

267   except the activity patterns.

268   **3.4 Impacts of disasters on anthropogenic activities**

269 This study accounted for the adaptability or adjustment behavior of residents to disasters during

270 the disaster event. The type of activity and its sensitivity to disaster affected the residents' disaster

271 response behavior. Recreation and shopping activities were easier to cancel and postpone than

272 work and study (*Cools et al., 2010*). The sensitivities of residents to disasters depended on their

273 socioeconomic characteristics and risk factors such as disaster- (flood-) related knowledge and

274 experience. People with higher education levels are more knowledgeable about disasters and are

275 more likely to receive early warning information and take effective measures (*Terti et al., 2015*).

276 Additionally, it is easier for workers to ignore the risks of a disaster (*Ruin et al., 2007*; *Drobot et*

277 *al., 2007*). Therefore, this study accounted for the impacts of education level on the response

278 behavior of residents to disaster events.

279 The impacts of a disaster on population distribution were determined by defining different activity

280 patterns and their changing probabilities. Figure 5 shows activity patterns during different disaster

281 scenarios for employed adult men who had received higher education. The "bad weather" scenario

282 was similar to the "daily activity" pattern. For instance, the change in travel probability during

283 "bad weather" due to a rainstorm reflected the adaptive behavior of residents. The "warning"

284 scenario assumed that the government had issued early warning information at 8 a.m., that schools

285 had suspended classes on weekdays, and the resident responses were stronger than those to the

286 "bad weather" scenario, thereby resulting in a greater difference in activity patterns.

287 **3.5 Dynamic exposure assessment**

288 The dynamic exposure was calculated based on the simulations of spatio-temporal distributions of

289 the population and flooding. Therefore, the exposure at each moment was calculated according to

290 the population distribution and flood data at that time. Based on the data availability, this study

291 focused only on three types of disaster-hit bodies, i.e., population, roads, and buildings.

292 (i) Population

293 Population exposure generally refers to the population exposed to the impacts of disaster events

294 and is characterized by regional population size or density. This study selected the exposed

295 population and accounted for vulnerable groups and road users. Age was the primary factor

296 impacting vulnerability. Specifically, the young (people under the age of 18 years) and the elderly

297 (people over 60 years old) were the vulnerable groups.

298 (ii) Roads

299 As the basic skeleton of a city, roads are not only the media for daily travel of passengers and

300 freight transportation but also disaster-hit bodies (*Yin, et al., 2016a*), as they are vulnerable to flood

301 disasters. This study selected the number and lengths of exposed roads to reflect road exposure.

302 (iii) Buildings

303 Aggravation of urban flooding has made building flooding more common in urban areas, resulting

304 in loss of internal property and construction structure. Additionally, the dynamic state of building

305 exposure is related to the safety of both the building as well as the surrounding population. In this

306 study, the area of the exposed building and the depth of accumulated water in the building were

307 considered as the building exposure.

308 **3.6 Scenario design**

309 The daily behaviors of people are characterized by certain patterns with regard to daily, weekly,

310 monthly, and annual cycles. The rainstorm ("bad weather") and disaster response measures

311 adopted by the organization ("warning") are likely to affect people's daily behaviors. Therefore,

312 12 scenarios, representing different flooding types and human activities, were designed in this

313 study (Table 3). S1, S2, S7, and S8 were control groups that indicated human activity with no rain

314 and no warning, while the rest of the scenarios were experimental groups.

315 **3.7 Model implementation and parameter setting**

316 As an important spatial data management and analysis technology, GIS plays an important role in

317 dynamic exposure analysis of urban floods. Because of the simplicity, readability and extensibility

318 of the Python programming language, an increasing number of research institutes are adopting it

319 for development. Therefore, the model was developed using the Visual Studio Code software

320 (*Visual studio code, 2018*) and Python programming language (*Python, 2018*). The development

321 of the graphical user interface (GUI), GIS module, and drawing module was realized by Qt (*Qt,*

322 *2018*), Geopandas (*Geopandas, 2018*), and Matplotlib (*Matplotlib, 2018*), respectively.

323 (i) Block generation

324 Blocks are irregular vector units whose size represents spatial resolution. Therefore, the spatial

325 resolution of the results is related to the study area and data. In this study, the study area was

326 divided into 237 blocks based on the method introduced in Sect. 3.3, with a minimum area of

327 2731.64 square meters. The block types and their spatial distributions are shown in Fig. 6 and Fig.

328 7, respectively. Most of the blocks in the study area were categorized as residential area, while

329 blocks of recreational areas were few and concentrated.

330 (ii) Parameter setting

331   To reduce the number of agent types, only a limited number of agent classes were used. The

332   distribution of population characteristics for Liandu District is shown in Table 4. The agents were

333   divided into 18 types for normal daily (non-disaster) scenarios (S1, S2, S7, and S8) and 24 types

334   for disaster scenarios (other scenarios except S1, S2, S7, and S8) based on the influence of

335   education level on the individual disaster response behavior (Fig. 8).

336   Since the census did not identify individuals according to addresses, at the start of each simulation,

337   an agent population with the same distributions of age, gender, employment, education level, and

338   travel mode was randomly located within the residential area for the case study. The synthetic

339   daily routines were described in probabilistic terms to capture the variability in the travel survey

340   and uncertainties in behavior. The probabilities of agents' daily activities were generated based on

341   the travel survey. We estimated the probabilities of all the activities of the population groups under

342   investigation.

343   (iii) Exposure threshold

344   Although flood fatalities can occur through a number of mechanisms, such as physical trauma,

345   heart attack, or electrocution, drowning accounts for two-thirds of the fatalities (*Jonkman and*

346   *Kelman, 2005*). Previous research has established that the probability of death or serious injury as

347   a result of exposure to flooding (*Abt et al., 1989*; *Karvonen et al., 2000*; *Lind et al., 2004*; *Jonkman*

348   *and Penning‐Rowsell, 2008*) is dominated by (1) the depth of floodwater and (2) the velocity of

349   floodwater. Additionally, the rate of water level rise can also play an important role in this regard.

350   However, other factors, such as age, fitness level, height, and weight of the individual, are also

351   important for determining their vulnerability to disasters. A comprehensive review of the flood-

352   related casualty data and methods to assess the risk of death or serious harm to people caused by

353 flooding is provided by the *Department for Environment Food and Rural Affairs and Environment*

354 *Agency (2003)* and *Jonkman and Penning‐Rowsell (2008)*. In this study, rather than predicting

355 mortality (which is subject to random factors as well as those mentioned previously), exposure to

356 floodwater depths of 25 cm or greater under relatively fast flowing (2.5 m/s or greater) conditions

357 was established as the threshold for the most vulnerable people (*DEFRA and Environment Agency,*

358 *2003*). This provided a conservative estimate of individuals vulnerable to floodwater rather than

359 an estimate of mortality (*Dawson et al., 2011*).

360 Since building steps (thresholds) exert a blocking effect on shallow flooding, they are likely to

361 reduce the degree of flooding by restricting the flood water to the outside of the building, thereby

362 reducing the exposure of the building. Therefore, this study assigned building step height to

363 corresponding block types according to the architectural design standards of China and the actual

364 conditions of the study area (Table 5). Therefore, the exposure of the building was determined

365 according to the depth of the flood and the height of the building steps. The depth of the water

366 entering the building was the difference between the depth of the flood and the height of the steps.

367 **4. Results**

368 **4.1 Flood simulation**

369 The temporal resolution of flood simulation results was unified with other output results for half

370 an hour. Figure 9 indicates the accumulated water depths and velocities of pluvial and fluvial

371 floods in the study area. As is evident, the pluvial and fluvial floods exerted significant impacts,

372 and the urban area near the Oujiang River was the most severely flooded. Additionally, water also

373 accumulated in the inner areas of the city, mainly on roads, in case of pluvial flood disasters. The

374 variations in water depth and velocity for seven severely flooded areas (including blocks and roads)

375   are presented in Fig. 10. As indicated, evident spatio-temporal variations in flooding were

376   observed. Figures 9 and 10 indicate that water depth was the main factor causing life and property

377   losses, whereas water velocity had little or no effect.

378   The flood simulation results were indirectly validated by actual water accumulation points. During

379   the 50-year flood in 2014, the city had 10 flooded roads and 18 water accumulation points. The

380   actual hydrological points selected according to the study area and the urban flooding results

381   simulated by the prototype system are indicated in Fig. 11.

382   To avoid overlapping with the simulated water accumulation results for roads, the actual flooding

383   points in the figure only included road junctions, and the entirety of Gucheng Road (Lutang Street

384   to Dayou Street section) and Liyang Street (which connected the senior middle school to the

385   Sanyan Temple section) was represented by corresponding intersection points. Figure 11 indicates

386   that both the simulation results and the actual water accumulation points were mainly distributed

387   along the river. The simulated water accumulation area (Fig. 11(a)) included roads in the center of

388   the city and was larger than the actual flooding area. This difference could be attributed to different

389   definitions of "water accumulation". The simulation results presented in Figure 11 included all

390   areas where the accumulated water depth during the flooding period was greater than 15 cm. The

391   actual water accumulation point was defined as one experiencing rainfall greater than 50 mm over

392   a 24 hour period. Additionally, it was characterized by the water accumulation depth of the road

393   reaching 15 cm (the meteorological department issued a blue rainstorm warning at this level), the

394   water withdrawal time reaching one hour, and the water accumulation scope value being greater

395   than 50 m^2. Certain gaps existed between the observational data and the actual river discharge

396   since the observation station was far from the study area. Hence, the results indicated that the

397   simulated water accumulation area during the fluvial flood (Fig. 11 (b)) was smaller than that of

398   the actual situation.

399   **4.2 Simulation of the spatio-temporal distribution of population**

400   The spatial and temporal resolutions of the modelling results could be adapted to the study area.

401   The area of the minimum block was 2731.64 m^2. The temporal resolution of the results was half

402   an hour, which could be set to 10 minutes or even 1 minute according to the requirements.

403   Additionally, no accurate traffic model was used to simulate agents' movements on road for two

404   reasons: (1) to improve efficiency and (2) we did not pay attention to high temporal-resolution

405   human movements (such as one minute or one second), but only focused on the population

406   distribution for a period of time, so the temporal resolution requirement of human activities was

407   low.

408   The spatio-temporal population distribution was simulated based on six scenarios: (1) daily,

409   weekday (S1, S7); (2) daily, weekend (S2, S8); (3) bad weather, weekday (S3, S9); (4) bad weather,

410   weekend (S4, S10); (5) warning, weekday (S5, S11); (6) warning, weekend (S6, S12). Figure 12

411   indicates the population variation for blocks and roads for the six scenarios. Figure 12(a) indicates

412   that, among the three weekend scenarios, the population in the playground (Block 77) changed

413   more than the population in the company (Block 113). Figure 12(b) indicates that the population

414   on the roads was volatile, and the morning peak hour during the weekend was delayed by an hour

415   in comparison to that during the weekdays. The population distribution in the study area is shown

416   in Fig. 13. The population was unevenly distributed and concentrated in recreational and

417   residential areas over the weekend. However, the population distribution on weekdays was

418   relatively uniform. The concurrent population distribution for the six scenarios changed

419   significantly during the weekend, while the distribution for weekdays changed little.

420   Figures 12 and 13 indicate that the population change patterns were different for different blocks

421   types. The daily routines of most people started from the residential area (home) in the morning,

422   followed by school or company blocks during weekdays and recreational areas during weekends,

423   and, finally, concluded with a return to the residential area at night. During the occurrence of

424   rainstorms or the reception of warning messages, different types of people reacted differently

425   (continuing, postponing, or cancelling the originally planned activities). Vulnerable people, such

426   as the elderly and children, and sensitive people, such as the homeless, were more likely to cancel

427   travel plans. Additionally, recreational activities were more likely to be cancelled than were study

428   and work activities.

429   The reliability of the simulation of the spatio-temporal population distribution was indirectly

430   verified by utilizing traffic flow data. Due to the lack of data for 2014, we used traffic flow data

431   from June 24 to July 7, 2017. The simulated total number of residents passing the four intersections

432   (such as the junction of the Liqing and Huayuan roads) and the actual measured traffic flow at the

433   intersections during the morning and evening peak hours on weekdays and weekends are shown

434   in Table 6 and Table 7. "Sim." means simulation results, and "Obs." means measured values which

435   are multi-day average results. "LQ" is Liqing Road, "KF" is Kaifa Road, "HY" is Huayuan Road,

436   "ZJ" is Zijin Road, and "LT" is Lutang Street. The deviation ratio was calculated as: (Sim - Obs)

437   / Obs.

438   In theory, the simulated value should be much larger than the measured value since the former

439   indicates the number of people while the latter represents the number of cars and buses. However,

440   as indicated in Table 6 and Table 7, the simulated value was close to the measured value. This

441   could be attributed to the assumption that the study area was closed and the simulated population

442   was the number of permanent residents, excluding the migrant population. In reality, the number

443   of migrants in the urban area during daytime is large owing to its geographical location. Moreover,

444   this study simplified human activities when simulating the spatio-temporal distribution of the

445   population. Therefore, the number of pedestrians on the road was small. However, there was a

446   deviation ratio of about ±5% between the simulated value and the measured value, except for three

447   deviation ratios of about ±10%. Therefore, the simulation method for the spatio-temporal

448   distribution of population is feasible, and the results are reliable.

449   **4.3 Dynamic exposure assessment**

450   Figure 14 presents the population exposure variation for two selected areas. The difference

451   between pluvial and fluvial flood scenarios could be attributed to differences in the changes and

452   degrees of water accumulation. Figure 14(a) indicates that population exposure was the highest for

453   the daily scenario, followed by the bad weather scenario and minimum warning scenario. However,

454   as indicated in Fig. 14(b), the population was most exposed to both weekend and weekday warning

455   scenarios. This is due to the assumption that the disaster response behavior adopted by residents

456   was to reduce travel, i.e., the refuge of residents was the residential area. Additionally, the response

457   was not based on the exposure of the residential area. Therefore, when residential areas, such as

458   Block 6, were exposed to floods, the residents chose to reduce travel, thus resulting in an increase

459   in the population of residential areas and consequently increasing the population exposure. Thus,

460   if the government informs the residents of Block 6 in advance about the location of appropriate

461   shelters, the exposed population will be effectively reduced. The method proposed in this study

462   can also help determine vulnerable populations and road users in the exposed blocks.

463   Figure 15 presents variations in the road and building exposures of two selected areas with serious

464   flooding. The road and building exposures for the study area are presented in Fig. 16. It can be

465   concluded that road and building exposures during pluvial and fluvial floods also varied with the

466   flood depth. Additionally, the exposed road length of the block fluctuated, while the buildings

467   were either entirely exposed or not exposed. Furthermore, the area of the road affected by pluvial

468   and fluvial floods was greater than that of the buildings. As indicated in Fig. 16, exposed buildings

469   were present only in a few areas (3 blocks for pluvial flood and 4 blocks for fluvial flood), while

470   roads were affected in several areas (19 blocks for pluvial flood and 15 blocks for fluvial flood).

471   In addition, buildings were the least exposed due to high thresholds or the number of building steps

472   designed and built in recent years, while roads and population were severely affected by floods.

473   **5. Discussion and conclusions**

474   Urban flooding considerably impacts the life of residents, in terms of both daily commuting and

475   casualties. This study proposed a method for obtaining high-resolution dynamic exposure to urban

476   flooding. First, the spatio-temporal distributions of pluvial and fluvial floods were simulated by

477   the LISFLOOD-FP model. Second, the responses of residents to bad weather and government

478   measures (warnings) were incorporated to develop an ABM to simulate residents' activities during

479   flooding. Finally, urban exposure during different flood scenarios was comprehensively simulated

480   and was based on the population and hydrological simulation results, road and building data, and

481   the case study of the Lishui urban district.

482   The proposed method can provide the government with high resolution dynamic exposure of

483   population, roads, and buildings to flooding along with information for urban vulnerability and

484   loss assessment, thus supporting the government disaster risk management. Additionally, it could

485   provide effective reference information for residents' travels. In summary, this study had four main

486 elements. First, different spatio-temporal distributions of water depth and velocity predictions were

487 obtained using the LISFLOOD-FP model. Second, an ABM was utilized to simulate the spatio-

488 temporal distributions of the population. Third, the impacts of pluvial and fluvial floods on

489 buildings were found to be small, while that on roads and the population was evident. Finally, if

490 residents simply reduced their travels (stayed at home), the exposure of the population in the

491 exposed residential areas increased.

492 It should be noted that there is no comprehensive way to verify the proposed method because

493 parameters of human behavior and psychological processes are difficult (or, to some extent,

494 impossible) to obtain. In this study, the proposed method was verified indirectly. The actual traffic

495 information for each road intersection was collected and compared with the simulated population

496 results. Additionally, the information for actual water accumulation points was compared with the

497 simulated water accumulation results.

498 However, a few limitations persist. For instance, considerable uncertainties regarding the use and

499 design of the ABM exist. These include differences in the responses of residents of the same type

500 to disasters in the same scenario. Therefore, based on the survey data, we designed simplified

501 activity patterns, which are consistent with the actual situation of the study area. Moreover,

502 simplification of the behavior patterns and disaster responses of residents is inevitable, resulting

503 in differences between the simulation results and reality.

504 Based on the analysis of the indirect validation results, we also found several problems. Since the

505 migrant population and the exchange between the city and the outside were not considered, the

506 simulated road population was small, so we needed to use real-time traffic data (such as taxi

507 trajectories and card data from public transportation) to calibrate activity patterns to obtain more

508 realistic population distribution results. Moreover, the actual water accumulation point information

509 cannot be completely consistent with the simulation result because of its definition, therefore the

510 simulation result can only be roughly verified. We need more abundant and accurate historical

511 hazard data to fine-tune the flood simulation results.

512 Our study focused more on the explorative method, while the result is just an application case. Due

513 to the limitation of the study area and data, the current results are quite general in an early stage.

514 The method proposed also has many areas in need of improvements, such as the design of ABM.

515 Therefore, future studies should focus on optimizing the proposed method and practical case

516 studies, which may produce more informative results.

517 **Acknowledgements**

518 This study was supported by the National Natural Science Foundation of China (Nos: 41771424,

519 41871299, 41631175) and National Key R & D Program of China (Nos: 2018YFB0505500,

520 2018YFB0505502). Dawei Han and Lu Zhuo were supported by Newton Fund via Natural

521 Environment Research Council (NERC) and Economic and Social Research Council (ESRC)

522 (NE/N012143/1).

523 **References**

524 Abt, S. , Wittier, R. , Taylor, A. and Love, D.: HUMAN STABILITY IN A HIGH FLOOD
525   HAZARD ZONE1. JAWRA Journal of the American Water Resources Association, 25:
526   881-890, https://doi.org/10.1111/j.1752-1688.1989.tb05404.x, 1989.

527 Atta-Ur-Rahman, D.: Disaster risk management, 2014.

528 Axelrod, R.: The complexity of cooperation: Agent-based models of competition and
529   collaboration (Vol. 3). Princeton University Press, 1997.

530 Bates, P. D., and De Roo, A. P. J.: A simple raster-based model for flood inundation simulation.
531   Journal of hydrology, 236(1-2), 54-77, https://doi.org/10.1016/S0022-1694(00)00278-X,
532   2000.

533 Bates, P., Trigg, M., Neal, J., Dabrowa ,A.: LISFLOOD-FP User manual, Code release 5.9.6,
534   School of Geographical Sciences, University of Bristol, University Road, Bristol, BS8 1SS,
535   UK, 2013. Available online at University of https://www.bristol.ac.uk/media-
536   library/sites/geography/migrated/documents/lisflood-manual-v5.9.6.pdf.

537 Bekhor, S., Ben-Akiva, M. E., and Ramming, M. S.: Evaluation of choice set generation
538   algorithms for route choice models. Annals of Operations Research, 144(1), 235-247,
539   https://doi.org/10.1007/s10479-006-0009-8, 2006.

540 Benenson, I., Omer, I., and Hatna, E.: Entity-based modeling of urban residential dynamics: the
541   case of Yaffo, Tel Aviv. Environment and Planning B: Planning and Design, 29(4), 491-
542   512, https://doi.org/10.1068/b1287, 2002.

543 Brunner, G. W.: HEC-RAS River Analysis System User's Manual Version 4.0. US Army Corps
544   of Engineers, Hydrologic Engineering Center. Report CPD-68, 2008.

545 Cen, G., Shen, J., and Fan, R.: Research on rainfall pattern of urban design storm. Advances in
546   Water Science, 9(1), 41-46, https://doi.org/10.14042/j.cnki.32.1309.1998.01.007, 1998.

547 Charley, W., Pabst, A., Peters, J.: The Hydrologic Modeling System (HEC-HMS): Design and
548   Development Issues. Hydrological Engineering Center, US Army Corps of Engineers,
549   Technical Paper No. 149, 1995.

550 Chen, Y., Zhou, H., Zhang, H., Du, G., and Zhou, J.: Urban flood risk warning under rapid
551   urbanization. Environmental research, 139, 3-10,
552   https://doi.org/10.1016/j.envres.2015.02.028, 2015.

553 Cools, M., Moons, E., Creemers, L., and Wets, G.: Changes in travel behavior in response to
554   weather conditions: do type of weather and trip purpose matter?. Transportation Research
555   Record: Journal of the Transportation Research Board, (2157), 22-28,
556   https://doi.org/10.3141/2157-03, 2010.

557 Danish Hydraulic Institute (DHI).: MIKE SHE Water movement user manual. DHI Water &
558   Environment, 2000.

559 Dankers, R., and Feyen, L.: Climate change impact on flood hazard in Europe: An assessment
560   based on high‐resolution climate simulations. Journal of Geophysical Research:
561   Atmospheres, 113(D19), https://doi.org/10.1029/2007JD009719, 2008.

562 Dawson, R. J., Peppe, R., and Wang, M.: An agent-based model for risk-based flood incident
563   management. Natural hazards, 59(1), 167-189, https://doi.org/10.1007/s11069-011-9745-4,
564   2011.

565 DEFRA and Environment Agency.: Flood risks to people phase 1: R&D Technical Report
566   FD2317. DEFRA, London, 2003.

567 Dijkstra, E. W.: A note on two problems in connexion with graphs. Numerische mathematik,
568   1(1), 269-271, 1959.

569 Drobot, S. D., Benight, C., and Gruntfest, E. C.: Risk factors for driving into flooded roads.
570   Environmental Hazards, 7(3), 227-234, https://doi.org/10.1016/j.envhaz.2007.07.003, 2007.

571 Gain, A. K., Mojtahed, V., Biscaro, C., Balbi, S., and Giupponi, C.: An integrated approach of
572   flood risk assessment in the eastern part of Dhaka City. Natural Hazards, 79(3), 1499-1530,
573   https://doi.org/10.1007/s11069-015-1911-7, 2015.

574 Geopandas: http://geopandas.org/, 2018.

575 Gilbert, N., and Troitzsch, K.: Simulation for the social scientist. McGraw-Hill Education (UK),
576   2005.

577 Guo, E., Zhang, J., Ren, X., Zhang, Q., and Sun, Z.: Integrated risk assessment of flood disaster
578   based on improved set pair analysis and the variable fuzzy set theory in central Liaoning
579   Province, China. Natural hazards, 74(2), 947-965, https://doi.org/10.1007/s11069-014-
580   1238-9, 2014.

581 Hammond, M. J., Chen, A. S., Djordjević, S., Butler, D., and Mark, O.: Urban flood impact
582   assessment: A state-of-the-art review. Urban Water Journal, 12(1), 14-29,
583   https://doi.org/10.1080/1573062X.2013.857421, 2015.

584 Havnø, K., Madsen, M. N., and Dørge, J.: MIKE 11–a generalized river modelling package.
585   Computer models of watershed hydrology, 733-782, 1995.

586 Horritt, M. S., and Bates, P. D.: Evaluation of 1D and 2D numerical models for predicting river
587   flood inundation. Journal of hydrology, 268(1-4), 87-99, https://doi.org/10.1016/S0022-
588   1694(02)00121-X, 2002.

589 Huang, H., Fan, Y., Yang, S., Li, W., Guo, X., Lai W., and Wang H.: A multi-agent based
590   theoretical model for dynamic flood disaster risk assessment. Geographical Research,
591   34(10):1875-1886, https://doi.org/10, 1875-1886, 10.11821/dlyj20151006, 2015.

592 IPCC.: Summary for Policymakers. In: Managing the Risks of Extreme Events and Disasters to
593   Advance Climate Change Adaptation. A Special Report of Working Groups I and II of the
594   Intergovernmental Panel on Climate Change. Cambridge University Press, Cambridge, UK,
595   and New York, NY, USA, pp. 3-21, 2012.

596 Johnstone, M. A.: Life safety modelling framework and performance measures to assess
597   community protection systems: application to tsunami emergency preparedness and dam
598   safety management, Ph.D. thesis, University of British Columbia, 2012.

599 Jonkman, S. N., and Kelman, I.: An analysis of the causes and circumstances of flood disaster
600   deaths. Disasters, 29(1), 75-97, https://doi.org/10.1111/j.0361-3666.2005.00275.x, 2005.

601 Jonkman, S. N., and Penning‐Rowsell, E.: Human Instability in Flood Flows 1. JAWRA
602   Journal of the American Water Resources Association, 44(5), 1208-1218,
603   https://doi.org/10.1111/j.1752-1688.2008.00217.x, 2008.

604 Kang, T., Zhang, X., Zhao, Y.,Wang, Y., and Zhang, W.: Agent-based Urban Population
605   Distribution Model. Scientia Geographica Sinica, 32(7): 90-797,
606   https://doi.org/10.13249/j.cnki.sgs.2012.07.003, 2012.

607 Karvonen, R. A., Hepojoki, A., Huhta, H. K., and Louhio, A.: The use of physical models in
608   dam-break analysis. RESCDAM Final Report. Helsinki University of Technology, Helsinki,
609   Finland, 2000.

610 Liang, Y., Wen, J., Du, S., Xu, H., and Yan J.: Spatial-temporal Distribution Modeling of
611   Population and its Applications in Disaster and Risk Management. Journal of
612   Catastrophology, 30(04):220-228, https://doi.org/ 10.3969/j.issn.1000-811X.2015.04.038,
613   2015.

614 Lind, N., Hartford, D., and Assaf, H.: Hydrodynamic models of human stability in a flood 1.
615   JAWRA Journal of the American Water Resources Association, 40(1), 89-96,
616   https://doi.org/10.1111/j.1752-1688.2004.tb01012.x, 2004.

617 Lindberg, S., Nielsen, J. B., and Carr, R.: An integrated PC-modelling system for hydraulic
618   analysis of drainage systems. In Watercomp'89: The First Australasian Conference on
619   Technical Computing in the Water Industry; Preprints of Papers (p. 127). Institution of
620   Engineers, Australia, 1989.

621 Lü, G., Batty, M., Strobl, J., Lin, H., Zhu, A. X., and Chen, M.: Reflections and speculations on
622   the progress in Geographic Information Systems (GIS): a geographic perspective.
623   International Journal of Geographical Information Science, 1-22,
624   https://doi.org/10.1080/13658816.2018.1533136, 2018.

625 Mahe, G., Paturel, J. E., Servat, E., Conway, D., and Dezetter, A.: The impact of land use change
626   on soil water holding capacity and river flow modelling in the Nakambe River, Burkina-
627   Faso. Journal of Hydrology, 300(1-4), 33-43, https://doi.org/10.1016/j.jhydrol.2004.04.028,
628   2005.

629 Mansur, A. V., Brondízio, E. S., Roy, S., Hetrick, S., Vogt, N. D., and Newton, A.: An
630   assessment of urban vulnerability in the Amazon Delta and Estuary: a multi-criterion index
631   of flood exposure, socio-economic conditions and infrastructure. Sustainability Science,
632   11(4), 625-643, https://doi.org/10.1007/s11625-016-0355-7, 2016.

633 Matplotlib: https://matplotlib.org/, 2018.

634 Moel, H. D., Aerts, J. C., and Koomen, E.: Development of flood exposure in the Netherlands
635   during the 20th and 21st century. Global Environmental Change, 21(2), 620-627,
636   https://doi.org/10.1016/j.gloenvcha.2010.12.005, 2011.

637 Nasiri, H., Mohd Yusof, M.J., and Mohammad Ali, T.A.: An overview to flood vulnerability
638   assessment methods. Sustain. Water Resour. Manag., 2: 331,
639   https://doi.org/10.1007/s40899-016-0051-x, 2016.Papinski, D., Scott, D. M., and Doherty,
640   S. T.: Exploring the route choice decision-making process: A comparison of planned and
641   observed routes obtained using person-based GPS. Transportation research part F: traffic
642   psychology and behaviour, 12(4), 347-358, https://doi.org/10.1016/j.trf.2009.04.001, 2009.

643 Parker, D., Fordham, M., Tunstall, S., and Ketteridge, A. M.: Flood warning systems under stress
644   in the United Kingdom. Disaster Prevention and Management: An International Journal,
645   4(3), 32-42, https://doi.org/10.1108/09653569510088050, 1995.

646 Python: https://www.python.org/, 2018.

647 Qt: https://www.qt.io/, 2018.

648 Ramming, M. S.: Network knowledge and route choice, Unpublished Ph. D. Thesis,
649   Massachusetts Institute of Technology, 2001.

650 Rossman, L. A.: Storm water management model user's manual Version 5.1 EPA-600/R-
651   14/413b[z]. National Risk Management Laboratory Laboratory Office of Research and
652   Development U. S. Environmental Protection Agency, 2015. Available online at
653   https://nepis.epa.gov/Exe/ZyPDF.cgi/P100N3J6.PDF?Dockey=P100N3J6.PDF

654 Röthlisberger, V., Zischg, A. P., and Keiler, M.: Identifying spatial clusters of flood exposure to
655   support decision making in risk management. Science of the total environment, 598, 593-
656   603, https://doi.org/10.1016/j.scitotenv.2017.03.216, 2017.

657 Ruin, I., Gaillard, J. C., and Lutoff, C.: How to get there? Assessing motorists' flash flood risk
658   perception on daily itineraries. Environmental hazards, 7(3), 235-244,
659   https://doi.org/10.1016/j.envhaz.2007.07.005, 2007.

660 Sallach, D. L., and Macal, C. M.: Introduction: The simulation of social agents. Social Science
661   Computer Review, 19(3), 245-248, https://doi.org/10.1177/089443930101900301, 2001.

662 Shabou, S., Ruin, I., Lutoff, C., Debionne, S., Anquetin, S., Creutin, J. D., and Beaufils, X.:
663   MobRISK: a model for assessing the exposure of road users to flash flood events. Natural
664   Hazards and Earth System Sciences, 17(9), 1631, https://doi.org/10.5194/nhess-17-1631-
665   2017, 2017.

666 Shi, P.: Theory and practice of disaster study. Journal of Natural Disasters, 4, 8-19, 1996.

667 Terti, G., Ruin, I., Anquetin, S., and Gourley, J. J.: Dynamic vulnerability factors for impact-
668   based flash flood prediction. Natural Hazards, 79(3), 1481-1497.
669   https://doi.org/10.1007/s11069-015-1910-8, 2015.

670 Visual studio code: https://code.visualstudio.com/, 2018.

671 Wan, H., Wang, J.: Analysis of Public Adaptive Behaviors to Drought and Flood Disasters in
672   Middle Reaches of Weihe River:A Case Study on Qishan County of Shaanxi Province. Acta
673   Agriculturae Jiangxi, https://doi.org/10.19386/j.cnki.jxnyxb.2017.05.21, 2017.

674 Weis, S. W. M., Agostini, V. N., Roth, L. M., Gilmer, B., Schill, S. R., Knowles, J. E., and
675   Blyther, R.: Assessing vulnerability: an integrated approach for mapping adaptive capacity,
676   sensitivity, and exposure. Climatic Change, 136(3-4), 615-629,
677   https://doi.org/10.1007/s10584-016-1642-0, 2016.

678 Werren, G., Reynard, E., Lane, S. N., and Balin, D.: Flood hazard assessment and mapping in
679   semi-arid piedmont areas: a case study in Beni Mellal, Morocco. Natural Hazards, 81(1),
680   481-511, https://doi.org/10.1007/s11069-015-2092-0, 2016.

681 Yang, X., Yue, W., and Gao, D.: Spatial improvement of human population distribution based on
682   multi-sensor remote-sensing data: an input for exposure assessment. International journal of
683   remote sensing, 34(15), 5569-5583, https://doi.org/10.1080/01431161.2013.792970, 2013.

684 Yin, Z.: Research of urban natural disaster risk assessment and case study, Ph.D. thesis, East
685   china normal university, Shanghai, China, 2009.

686 Yin, J., Yu, D., and Wilby, R.: Modelling the impact of land subsidence on urban pluvial
687   flooding: A case study of downtown Shanghai, China. Science of the Total Environment,
688   544, 744-753, https://doi.org/10.1016/j.scitotenv.2015.11.159, 2016a.

689   Yin, W., Yu, H., Cui, S., and Wang, J.: Review on methods for estimating the loss of life
690   induced by heavy rain and floods. Progress in Geography, 35(2), 148-158,
691   https://doi.org/10.18306/dlkxjz.2016.02.002, 2016b.

692   **Figure 1.** Location of the study area (left) and a digital elevation model indicating the specific
693   details of the study area (right).

694   **Figure 2.** Overview of the dynamic exposure simulation to urban flooding.

695   **Figure 3.** Rainfall simulation results based on the CHM method, and observational data used for
696   fluvial flood simulation.

697   **Figure 4.** A synthetic daily routine generated from the travel survey and census data for an
698   employed male agent aged 18–60 years.

699   **Figure 5.** Activity patterns for an employed male agent aged 18–60 years and highly educated
700   during disaster scenarios. (a) Bad weather (weekday) (b) Warning (weekday) (c) Bad weather
701   (weekend) (d) Warning (weekend).

702   **Figure 6.** Block numbers of different block types.

703   **Figure 7.** Spatial distribution of blocks.

704   **Figure 8.** Agent types for daily and disaster scenarios. Daily scenarios refer to S1, S2, S7, and S8.
705   Others are disaster scenarios.

706   **Figure 9.** Map of accumulated water depths and velocities. T means time here.

707   **Figure 10.** Changes in the surface water depths and velocities for eight severely flooded areas.
708   The "dep" indicates water depth, and "vel" indicates water velocity.

709   **Figure 11.** Map of the flooded area indicating the flooding simulation and the real flood in 2014.
710   The information for the flooded area was provided by Lishui City Housing and Urban-Rural
711   Construction Bureau.

712   **Figure 12.** Population changes in blocks and roads for the six scenarios.

713   **Figure 13.** Population distribution for the six scenarios. T means time here.

714   **Figure 14.** Changes in the population exposure of two blocks for the 12 scenarios. Block 168 was
715   a recreational area, and Block 6 was a residential area.

716   **Figure 15.** Changes in road and building exposures in severely flooded blocks. The exposed road

717   length and building area represent road and building exposures, respectively.

718   **Figure 16.** Map of road and building exposures. T means time here.

719
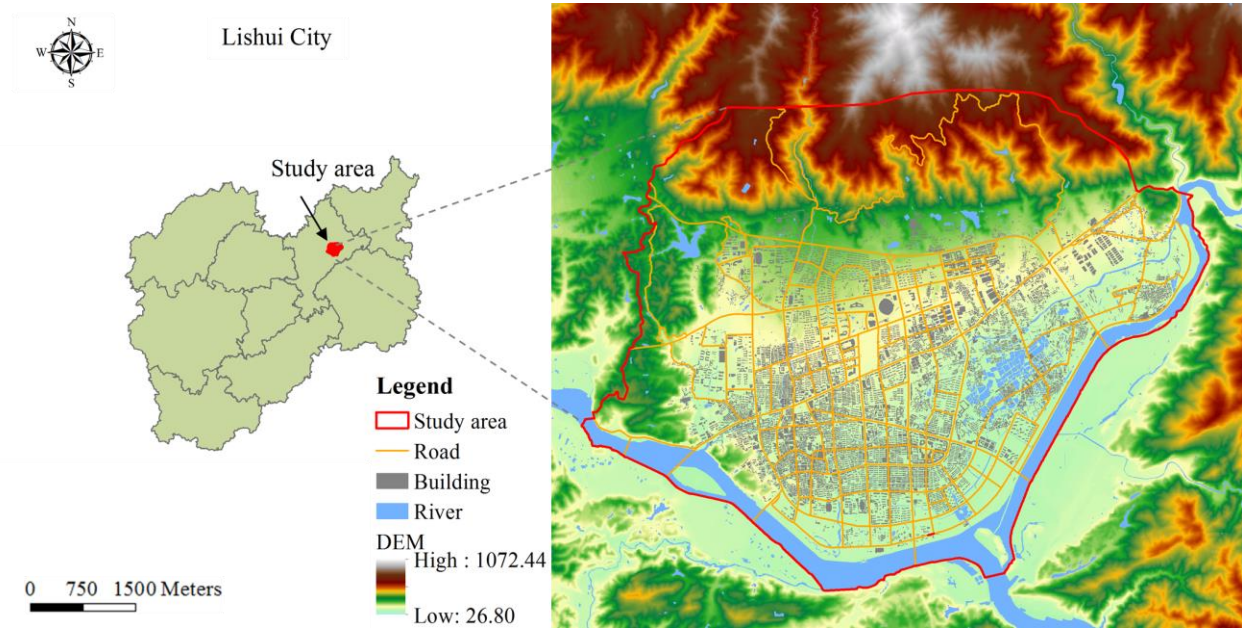
720

721 **Figure 1.** Location of the study area (left) and a digital elevation model indicating the specific
722 details of the study area (right).
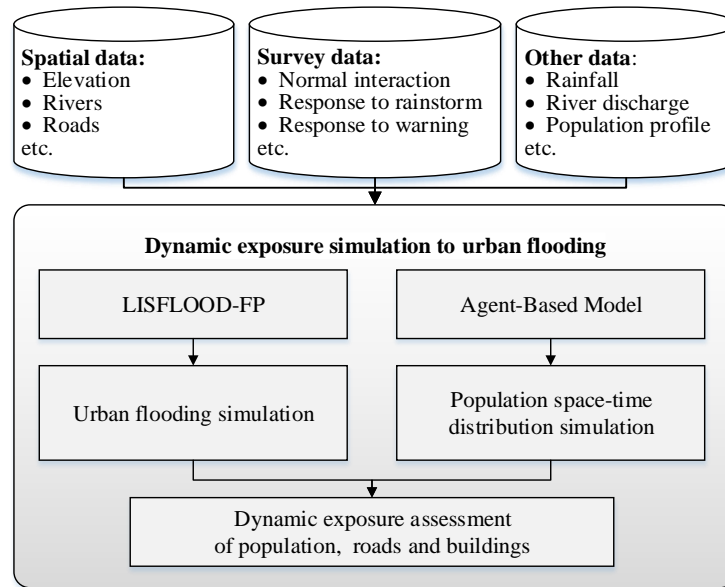
723

724   **Figure 2.** Overview of the dynamic exposure simulation to urban flooding.

725
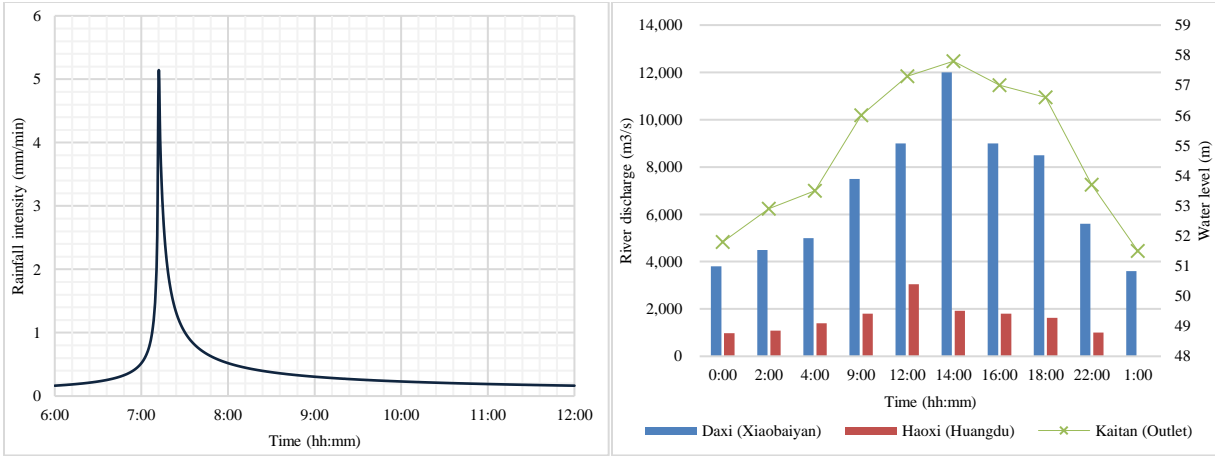
726   (a) Rainfall simulation data   (b) Observational data

727 **Figure 3.** Rainfall simulation results based on the CHM method, and observational data used for

728 fluvial flood simulation.

729

730   (a) Activity on weekdays   (b) Activity on weekends

731 **Figure 4.** A synthetic daily routine generated from the travel survey and census data for an

732 employed male agent aged 18–60 years.

733

734   (a) Bad weather (weekday)   (b) Warning (weekday)

735
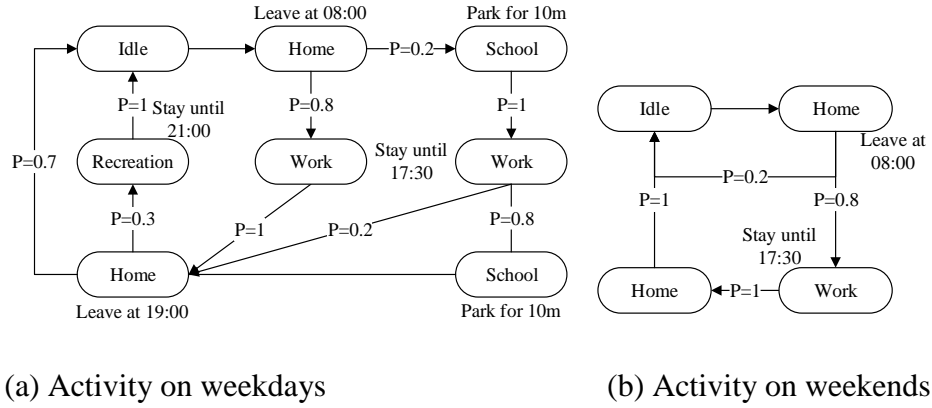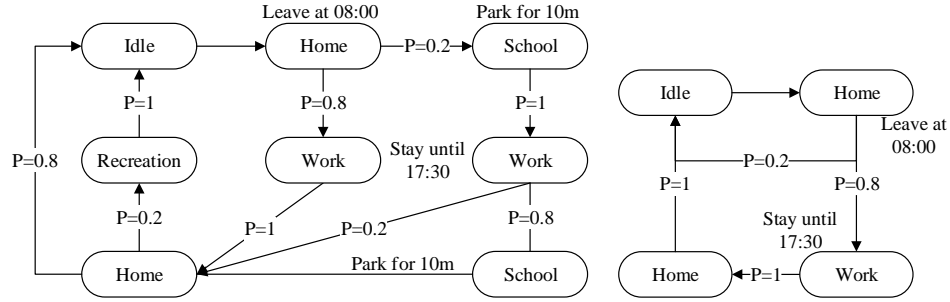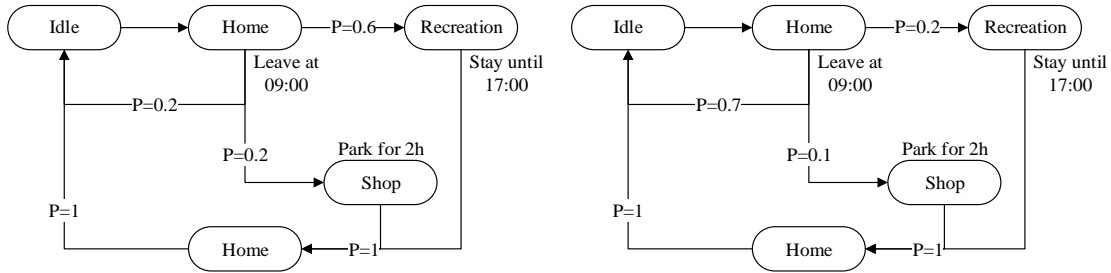
736   (c) Bad weather (weekend)   (d) Warning (weekend)

737 **Figure 5.** Activity patterns for an employed male agent aged 18–60 years and highly educated

738 during disaster scenarios. (a) Bad weather (weekday) (b) Warning (weekday) (c) Bad weather

739 (weekend) (d) Warning (weekend).

740
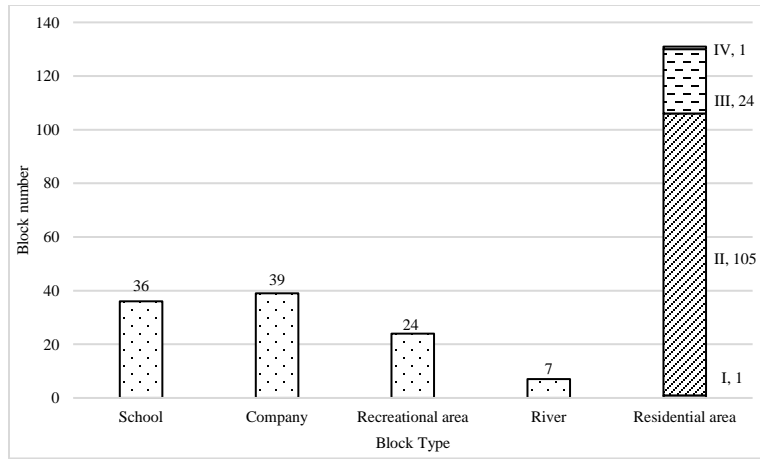
741

742   **Figure 6.** Block numbers of different block types.

743

Figure 7. Spatial distribution of blocks.

745

746
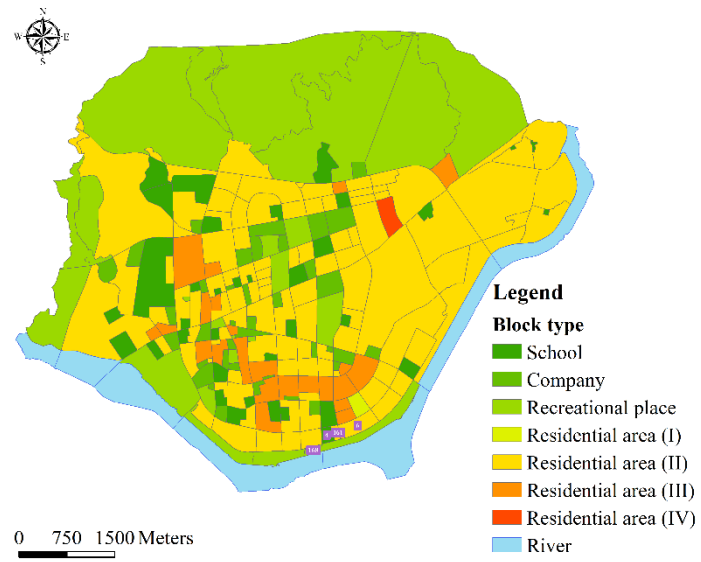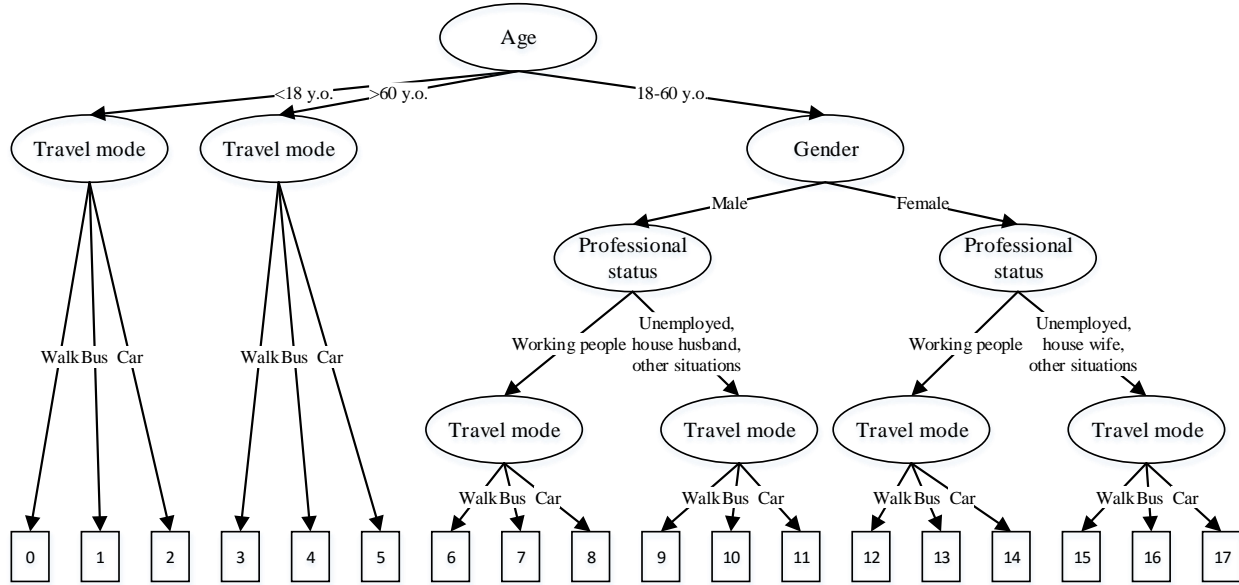
747 (a) Agent types for daily scenarios

748
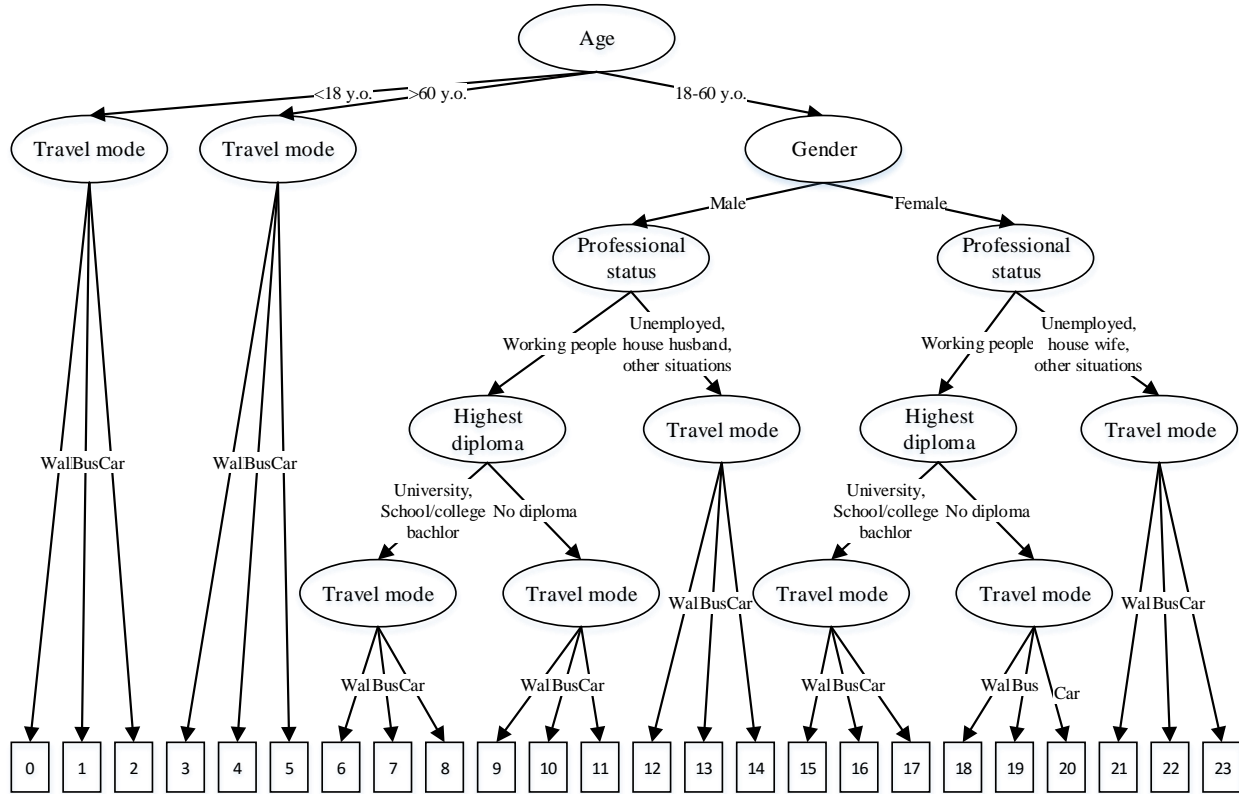
749 (b) Agent types for disaster scenarios

750 **Figure 8.** Agent types for daily and disaster scenarios. Daily scenarios refer to S1, S2, S7, and

751 S8. Others are disaster scenarios.

752
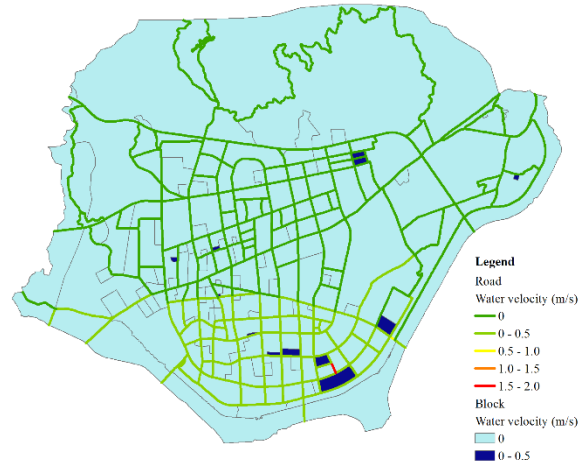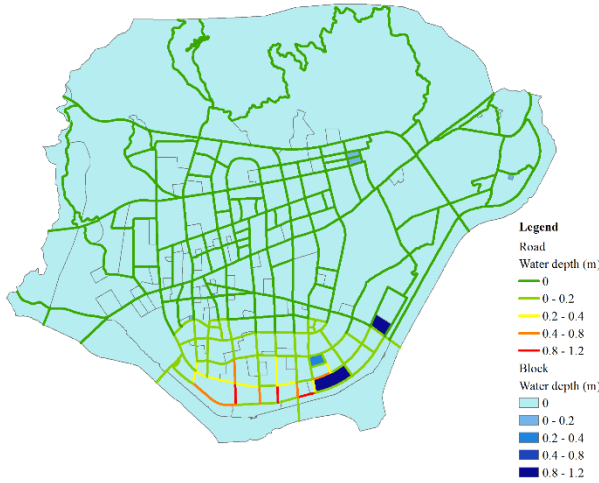
753   (a) Water depth (pluvial flood, T = 15:00)   (b) Water velocity (pluvial flood, T = 08:00)

754
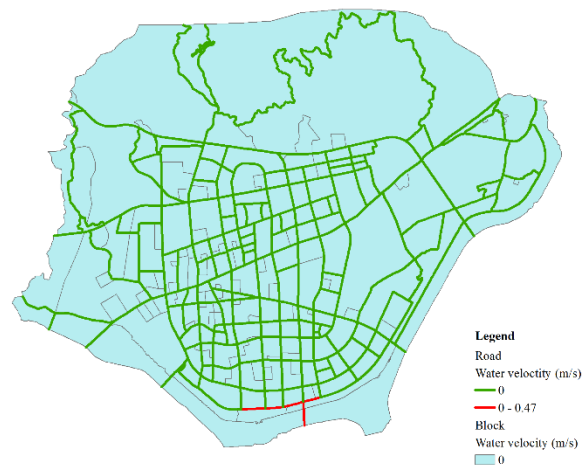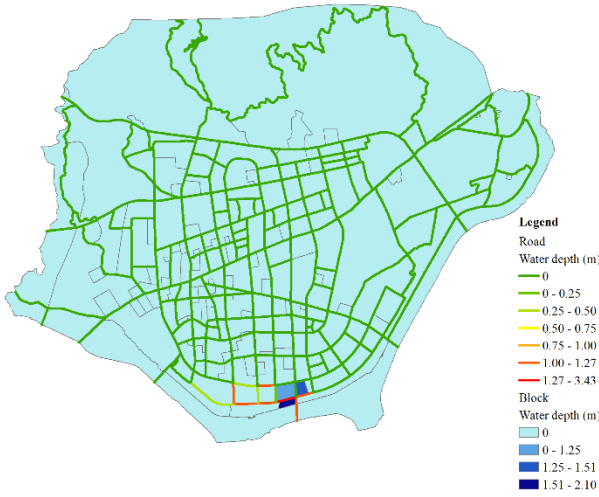
755   (c) Water depth (fluvial flood, T = 16:00)   (d) Water velocity (fluvial flood, T = 16:00)

756   **Figure 9.** Map of accumulated water depths and velocities. T means time here.

757

758   (a) Pluvial flood   (b) Fluvial flood

759   **Figure 10.** Changes in the surface water depths and velocities for eight severely flooded areas.

760   The "dep" indicates water depth, and "vel" indicates water velocity.

761
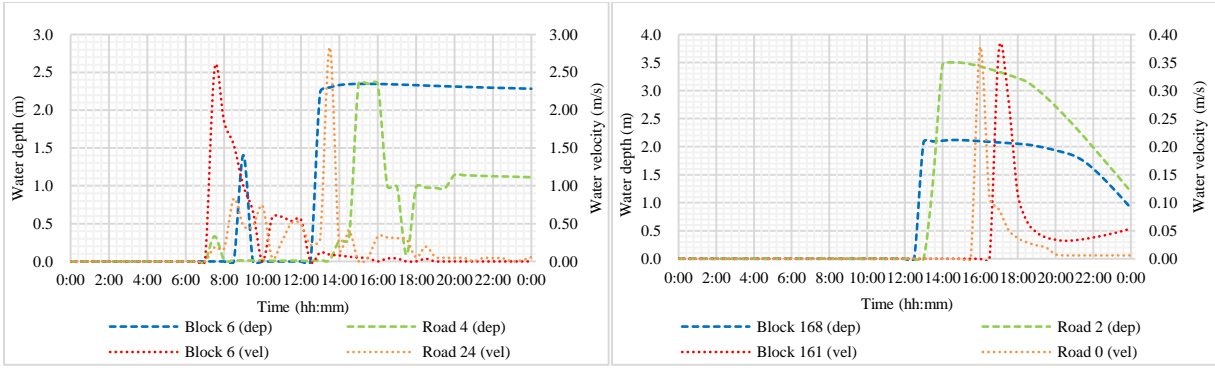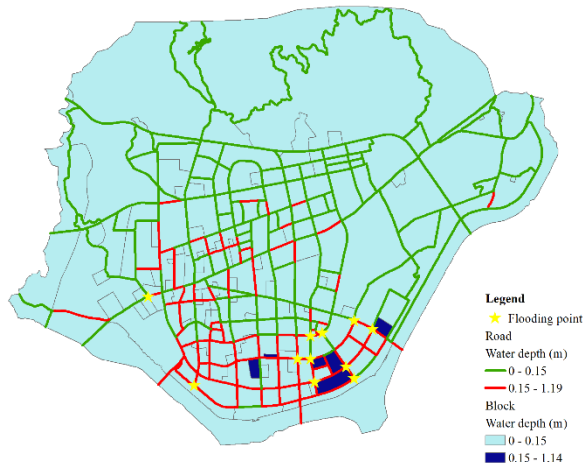
762   (a) Pluvial flood   (b) Fluvial flood
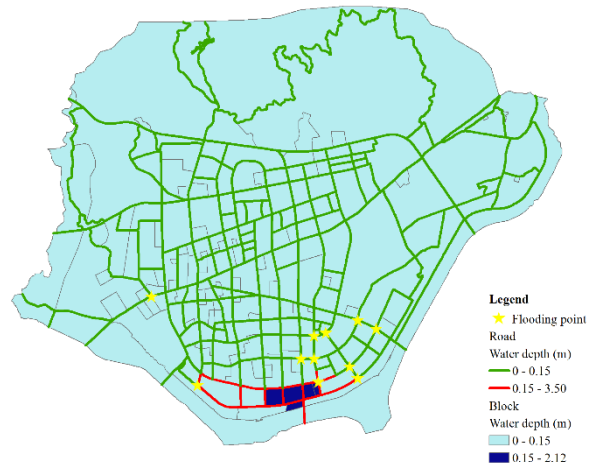
763 **Figure 11.** Map of the flooded area indicating the flooding simulation and the real flood in 2014.

764 The information for the flooded area was provided by Lishui City Housing and Urban-Rural

765 Construction Bureau.

766

767   (a) Block   (b) Road

768   **Figure 12.** Population changes in blocks and roads for the six scenarios.

769
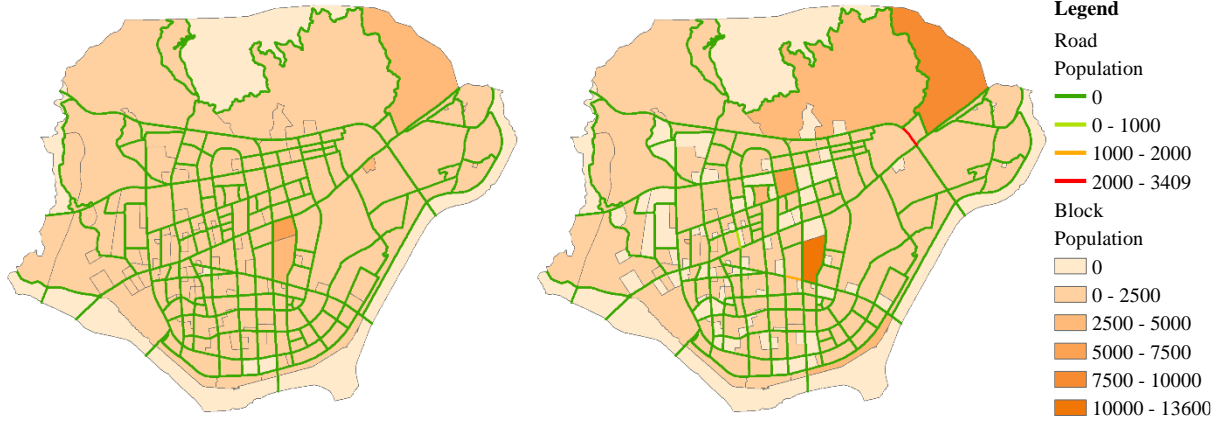
770   (a) Daily, weekday (T = 09:00)   (b) Daily, weekend (T = 09:00)

771
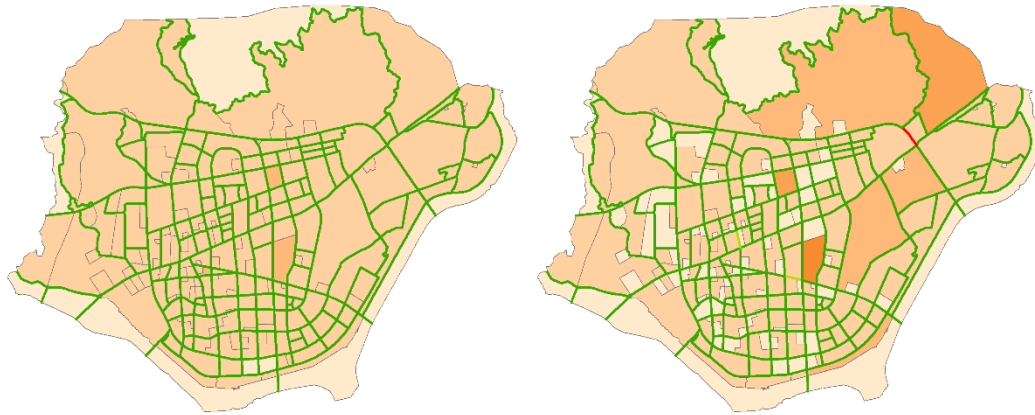
772   (c) Bad weather, weekday (T = 09:00)   (d) Bad weather, weekend (T = 09:00)

773
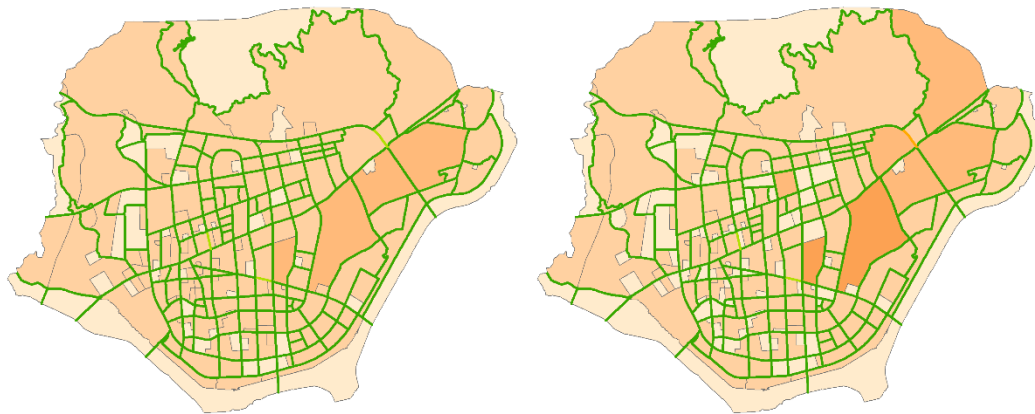
774   (e) Warning, weekday (T = 09:00)   (f) Warning, weekend (T = 09:00)

775   **Figure 13.** Population distribution for the six scenarios. T means time here.

776

777
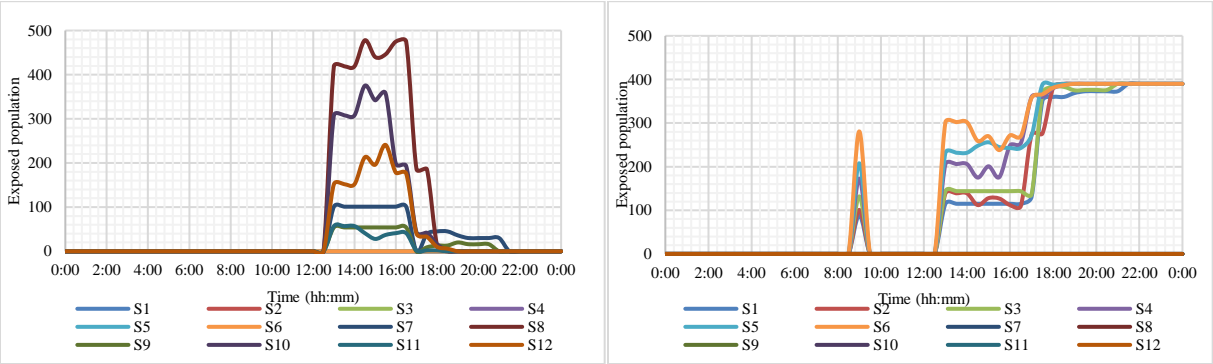
778   (a) Population exposure (Block 168)   (b) Population exposure (Block 6)

779   **Figure 14.** Changes in the population exposure of two blocks for the 12 scenarios. Block 168

780   was a recreational area, and Block 6 was a residential area.

781
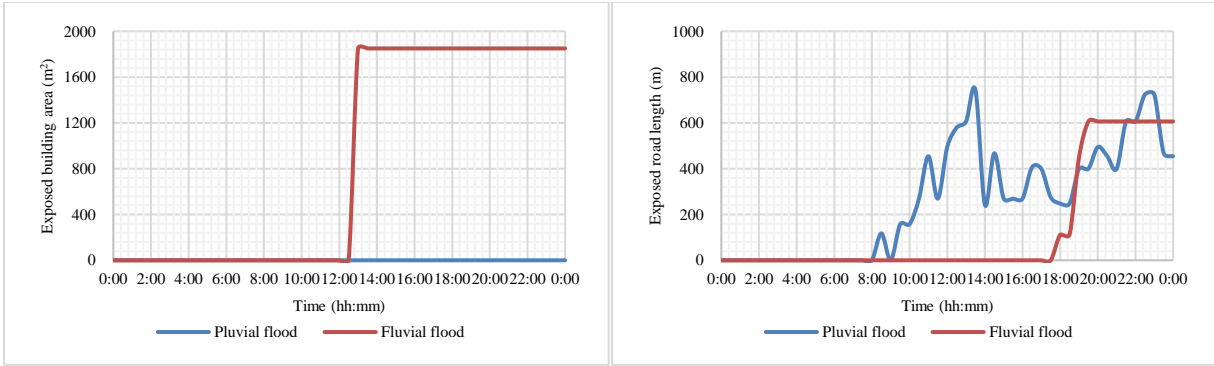
782   (a) Exposed building area (Block 168)   (d) Exposed road length (Block 6)

783   **Figure 15.** Changes in road and building exposures in severely flooded blocks. The exposed road

784   length and building area represent road and building exposures, respectively.

785
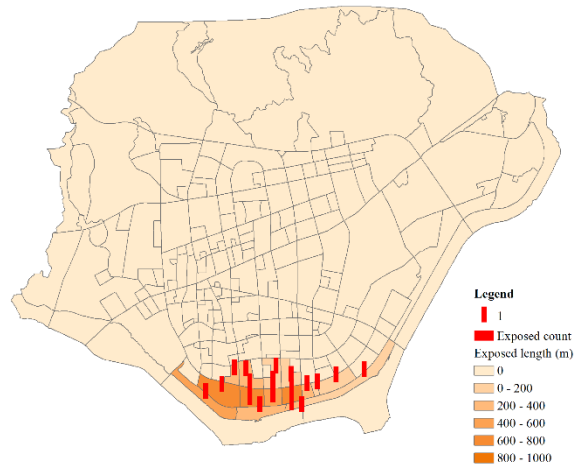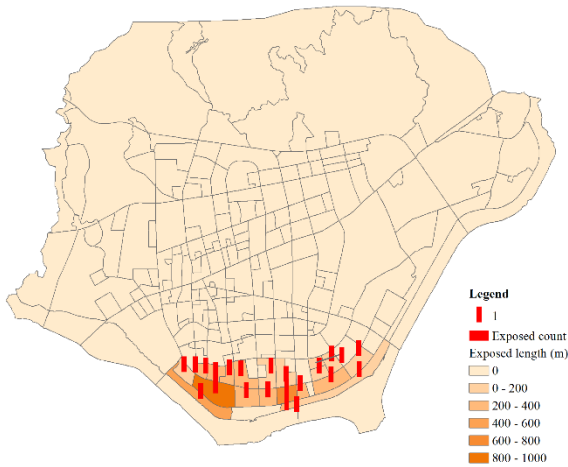
786   (a) Road exposure (pluvial flood, T = 18:30)   (b) Road exposure (fluvial flood, T = 18:30)

787
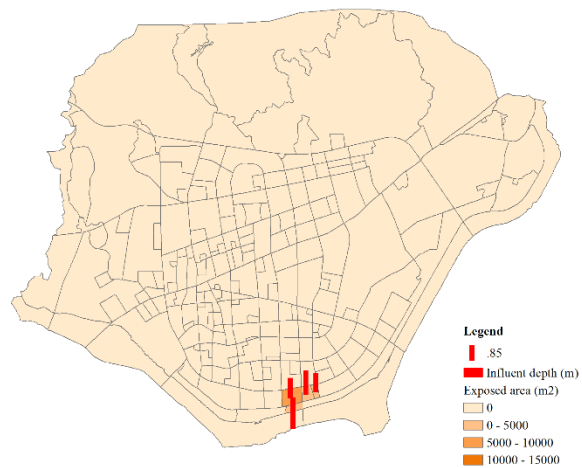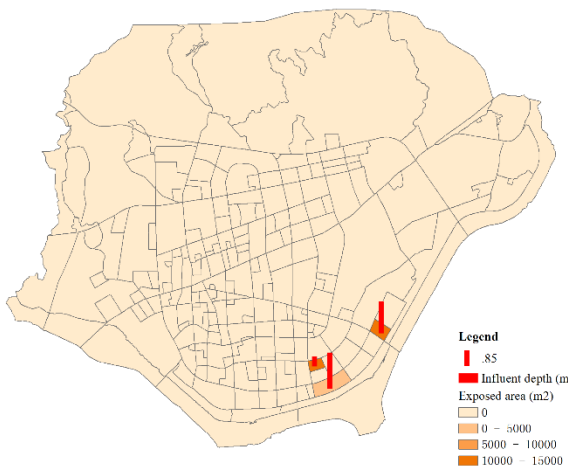
788   (c) Building exposure (pluvial flood, T = 18:30) (d) Building exposure (fluvial flood, T = 18:30)

789   **Figure 16.** Map of road and building exposures. T means time here.

790 **Table 1** Data used in this study.

791 **Table 2.** Parameter values for the rainstorm intensity formula.

792 **Table 3.** Parameter variations used in the simulation scenarios.

793 **Table 4.** Sociodemographic characteristics of the study area population.

794 **Table 5.** Building step heights for different block types.

Table 6. Traffic flow and population simulation results during peak hours on weekdays.

Table 7. Traffic flow and population simulation results during peak hours on weekends.

795   **Table 1.** Data used in this study.

Data	Source	Time	Use
Digital elevation model	Local government	2013	Topography (regular square grids with a 5 m resolution)
Basic geographic data	Local government	2015	Locations of rivers, roads, and buildings
Hydrological data	Local government	Aug 20, 2014	River discharge and water level
1 km grid population data	National Earth System Science Data Sharing Infrastructure, National Science & Technology Infrastructure of China (http://www.geodata.cn)	2010	Number of residents per grid in the study area
Population profile	Lishui Statistical Yearbook and Liandu Yearbook (http://tjj.lishui.gov.cn)	2014	Gender, age, education level, employment, and travel mode profiles were used to classify agent groups
Travel survey data	Face-to-face questionnaire surveys	July 8, 2018 to July 14, 2018	Social characteristics and daily activities of 500 residents
Traffic flow data	Local government	June 24, 2017 to July 7, 2017	Number of vehicles passing through a node within one hour at four intersections from June 24, 2017 to July 7, 2017 in this area
Water accumulation points	Local government (http://www.zjjs.com.cn)	Aug 20, 2014	Location

796

797 **Table 2**. Parameter values for the rainstorm intensity formula.

Parameter	Value
A	1265.3
b	5.919
c	0.587
n	0.611

798

799   **Table 3**. Parameter variations used in the simulation scenarios.

Scenarios	Flooding type	Human behavior	Weekdays or weekends
S1	Pluvial flood	Daily	Weekdays
S2	Pluvial flood	Daily	Weekends
S3	Pluvial flood	Bad weather	Weekdays
S4	Pluvial flood	Bad weather	Weekends
S5	Pluvial flood	Warning	Weekdays
S6	Pluvial flood	Warning	Weekends
S7	Fluvial flood	Daily	Weekdays
S8	Fluvial flood	Daily	Weekends
S9	Fluvial flood	Bad weather	Weekdays
S10	Fluvial flood	Bad weather	Weekends
S11	Fluvial flood	Warning	Weekdays
S12	Fluvial flood	Warning	Weekends

800

801   **Table 4**. Sociodemographic characteristics of the study area population.

Variables	Groups	Percentage (%)
Gender	Male	50.43
	Female	49.57
Age	0-17	18.73
	18-60	63.34
	>60	17.93
Professional status	Employed	55.77
	Unemployed	44.23
Education level	University, school-college, bachelor	14.46
(Highest diploma)	No diploma	85.54
Travel mode	Walk	25.24
	Bus	43.06
	Car	31.70

802   Note: Data are drawn from the 2015 Lishui Statistical Yearbook and 2015 Liandu Yearbook.

Table 5. Building step heights for different block types.

No	Block type	Building type	Building step height
1	Residential area I	Garden house, villa	0.35 m (with > 9 floors, 0.60 m)
2	Residential area II	High-rise apartments and new village houses (before 1988); new residential quarters and commercial houses (after 1988)	0.35 m (with > 9 floors, 0.60 m)
3	Residential area III	New and old lane homes, three types of staff housing	0.10 m
4	Residential area IV	Shed house	0.05 m
5	School	Educational building	0.35 m (with > 9 floors, 0.60 m)
6	Company	Office building	0.35 m (with > 9 floors, 0.60 m)
7	Recreational area	Public buildings for business, culture, sports, and other uses	0.35 m (with > 9 floors, 0.60 m)

803

Table 6. Traffic flow and population simulation results during peak hours on weekdays.

Road junction	Time	Sim.	Obs.	Deviation ratio
LQ-KF	8:00–9:00	319	366	-12.84%
LQ-KF	17:00–18:00	602	591	1.86%
LQ-HY	8:00–9:00	353	398	-11.31%
LQ-HY	17:00–18:00	740	731	1.23%
LQ-ZJ	8:00–9:00	381	369	3.25%
LQ-ZJ	17:00–18:00	824	814	1.23%
LT-ZJ	8:00–9:00	531	508	4.53%
LT-ZJ	17:00–18:00	994	938	5.97%

804

Table 7. Traffic flow and population simulation results during peak hours on weekends.

Road junction	Time	Sim.	Obs.	Deviation ratio
LQ-KF	8:00–9:00	523	529	-1.13%
LQ-KF	17:00–18:00	659	693	-4.91%
LQ-HY	8:00–9:00	761	725	4.97%
LQ-HY	17:00–18:00	822	790	4.05%
LQ-ZJ	8:00–9:00	651	638	2.04%
LQ-ZJ	17:00–18:00	825	873	-5.50%
LT-ZJ	8:00–9:00	778	712	9.27%
LT-ZJ	17:00–18:00	1083	1132	-4.33%

805